Materials Science Forum
ISSN: 1662-9752, Vol. 1089, pp 71-79
doi:10.4028/p-026sj4

Submitted: 2022-09-10
Revised: 2022-10-24
Accepted: 2022-11-25
Online: 2023-05-26

Evaluation of Crystal Quality and Dopant Activation of Smart Cut™- Transferred 4H-SiC Thin Film

Guillaume Gelineau[1,a*], J. Widiez[1,b], E. Rolland[1c], K. Vladimirova[1,d], A. Moulin[1,e], V. Prudkovskiy[1,f], N. Troutot[1g], P. Gergaud[1,h], D. Mariolle[1,i], S. Barbet[1,j], V. Amalbert[1,k], G. Lapertot[2,l], K. Mony[2,m], S. Rouchier[3,n], R. Boulet[3,o], G. Berre[3,p], Walter Schwarzenbach[3,q] and Y. Bogumilowicz[1,r]

[1] Univ. Grenoble Alpes, CEA, Leti, F-38000 Grenoble, France

[2]Univ. Grenoble Alpes, CEA, Grenoble INP, IRIG, PHELIQS, 38000 Grenoble, France

[3]Soitec SA, Chemin des Franques, 38190 Bernin, France

[a]guillaume.gelineau@cea.fr, [b]julie.widiez@cea.fr, [c]emmanuel.rolland@cea.fr, [d]krenema.vladimirova@cea.fr, [e]alexandre.moulin@cea.fr, [f]vladimir.prudkovskiy@cea.fr, [g]nicolas.troutot@cea.fr, [h]patrice.gergaud@cea.fr, [i]denis.mariolle@cea.fr, [j]sophie.barbet@cea.fr, [k]vincent.amalbert@cea.fr, [l]gerard.lapertot@cea.fr, [m]karine.mony@cea.fr, [n]severin.rouchier@soitec.com, [o]romain.boulet@soitec.com, [p]guillaume.berre@soitec.com, [q]walter.schwarzenbach@soitec.com, [r]yann.bogumilowicz@cea.fr

Keywords: SiC layer transfer, Smart Cut™, crystal quality, dopant activation, Raman spectroscopy.

Abstract. The Smart Cut™ process offers an advantageous opportunity to provide a large number of performance-improved SiC substrates for power electronics. The crystalline quality and the electrical activation of the 4H-SiC transferred layer are then at stake when it comes to the power device reliability. In this study, we find that the H^+ ion implantation used for the Smart Cut™ process leads to electrical deactivation of dopants and partially disorders the material. The transferred layer fully recovers its initial crystalline quality after a 1300°C anneal, with no further evolution beyond this temperature. At this point however, the *n*-type dopants are still inactive. The dopant reactivation occurs in the same temperature range than that of implanted nitrogen: between 1400°C and 1700°C. After 1700°C, the initial doping level of bulk SiC is recovered.

Introduction

Recent restrictions on combustion-engine vehicles sells for 2035 and beyond from the European Union [1] encouraged expert analysts to predict the market shares of electric vehicles, and thus of power silicon carbide (SiC) modules, to skyrocket in the next few years [2]. Despite the continuous improvement of substrates quality over the years, as well as an always more important number of manufacturers, a global SiC wafer shortage is feared among the community, as the production ramp up from 6" to 8" wafer size is still to be effective. In this extent, the Smart Cut™ process offers a state-of-the art opportunity to overcome this challenge. Significant yield optimization and performance improvements have been achieved by combining the benefits of an ultra-low resistivity polycrystalline handle and of a high quality 4H-SiC transferred layer [3]. The crystalline quality and the electrical activation of the 4H-SiC transferred layer are then at stake when it comes to the power device reliability. The H^+ ion implantation used for the Smart Cut™ process however leads to electrical deactivation and partially disorders the material. Annealing is then mandatory to recover all the properties of the transferred layer. The absence of any buried thermal oxide in such so-called SmartSiC™ substrates – which was the key feature in the case of Silicon On Insulator (SOI)-based products [4] – allowed us to investigate the recovery of the transferred layer over uncommonly high temperatures, using various characterization techniques. Particularly, the study of the Raman Longitudinal Optic Plasmon-Coupled (LOPC) mode is of great interest, since the position and shape of this peak can be directly related to the carrier concentration of a polar semiconductor such as SiC [5], [6]. In this paper, we present for the first time studies over a broad range of temperature (from

RT to 1900°C), allowing to analyze the entire progress of crystal recovery: starting from the evolution of the crystallinity of the implanted and then transferred material, to its dopant reactivation.
Although that Rutherford Backscattering Spectroscopy (RBS) in channeling mode is the most common method to characterize implantation damage, it is often quite costly and cannot be conducted in clean room. In this extent, Raman spectroscopy offers more cost-friendliness and accessibility. This second technique is also widely used for damage and amorphization characterization after ion implantation [7]–[12]. Particularly, a disordered material will allow more degrees of freedom to its atoms due to the presence of vacancies. Consequently, the Raman response of a bi-atomic compound such as SiC will reflect the disorder through the apparition of broad bands, characteristic of the Raman-active Si-Si, Si-C or C-C disordered phonons. The amplitude of those can then be used to quantify the crystallinity of the material when compared to a pristine reference [7], [12].
Raman spectroscopy may as well come in useful for doping characterization in polar semiconductors such as InP or GaN or SiC [5], [6]. Indeed, at high carrier concentrations, longitudinal oscillations of the lattice will influence the material's electronic susceptibility through the effect of the modulation of the associated macroscopic electric field. A consequence of this effect is the coupling of the longitudinal Optic (LO) phonon with the plasmon. While some authors applied the model to 4H-SiC and 6H-SiC in order to, for instance, characterize the spatial repartition of *n*-type dopants in PVT-grown wafers [13]–[15] or to investigate the electrical activity of extended defects [16], no paper about dopant reactivation in transferred SiC thin film was found in the literature. The experimental data obtained in the context of the present study was fitted using the model described in [14] in order to retrieve the active donor concentration from the inferred plasmon frequency.
The dopant activation in silicon carbide is a widely studied phenomenon, as most manufacturers use N^+, P^+, Al^+, or B^+ ion implantations to process SiC power devices [17]. After implantation, annealing is mandatory – not only to recover a good crystalline quality; but also to make the impurities diffuse and become electrically active. The minimum temperature varies from one doping species to another. Particularly, 1650°C is a commonly accepted activation temperature for Al or N [17]–[22]. If such temperatures are well-known to be needed to activate implanted impurities, the reactivation of hydrogen-implanted *n*-doped 4H-SiC was barely studied beyond moderated temperatures of around 1300°C [4], [23]. In the case of Smart Cut™ layer transfer, the N electrical reactivation phenomenon might be associated to two distinct mechanisms. Either it is related to the N diffusion activation energy, as it is for post-implantation activation [17]. Or – if the path of the displaced N atom is sufficiently short – it may only come from the reconstruction of the disordered C lattice (since N is electrically active when substituted to a C atom [24]). In the last case, the activation temperatures might be rather different from those found by other research groups for implanted N [19].

Materials and Methods

In order to characterize both the crystal quality and its dopant reactivation, three series of samples were prepared as follows. 1- Commercial wafers of 4°-off axis, 4.10^{18} cm^{-3} N-doped bulk 4H-SiC were H^+-implanted as conventional SmartSiC™ substrates [3], before annealing up to 800°C for 30 minutes. This first series served for both crystallinity recovery (Raman, RBS) and dopant activation analysis. 2- Another series was prepared using a monocrystalline 4H-SiC layer, transferred on a monocrystalline 4H-SiC substrate using the same implantation process. This second series was then annealed at 950°C, 1300°C, 1500°C and 1700°C (30 minutes each), and was used for XRD and Spreading Scanning Resistance Microscopy (SSRM) characterizations. 3- A last series was prepared the same way as the second one, but transferred on a polycrystalline handle substrate instead of on a monocrystalline one, and annealed up to 1900°C. This last series allowed characterizing the dopant activation of the transferred layer up to high temperatures – taking advantage of the polySiC receiver, which does not show any Raman response in the 950-1050 cm^{-1} range (and thus allowing a clear reading of the transferred layer's LOPC mode only). All Raman spectra were acquired in backscattering geometry using a 532 nm laser excitation on a Renishaw IN-VIA apparatus with a numerical aperture of 0.9. The laser power was varied along the experiment to compensate for the loss of intensity of the LOPC mode with higher doping concentrations. It was prior verified that no

photocurrent was induced in the 4H-SiC layer with higher laser power. The channeled RBS spectra were performed with a AIFIRA-type particle accelerator [25], using a 2.8 MeV alpha particles beam. The damage quantification was carried out using the technique described in [26]. Eventually, the I-V measurements were performed on samples from the third series, using a coplanar c-TLM test structure with MESA insulations, forcing the current to flow across both the top layer and the handle substrate.

Implanted and Transferred Layer Crystal Quality

Bulk crystal recovery. Two observations can be made from the channeled RBS spectra displayed on Fig. 1. First, it is hardly possible to distinguish any difference between the silicon backscattering spectra from the as implanted and the 200°C anneal samples. Then, the amplitude of the peak from the sample annealed at 600°C decreases drastically – testifying of the important recovery of the crystal over this range of temperature.

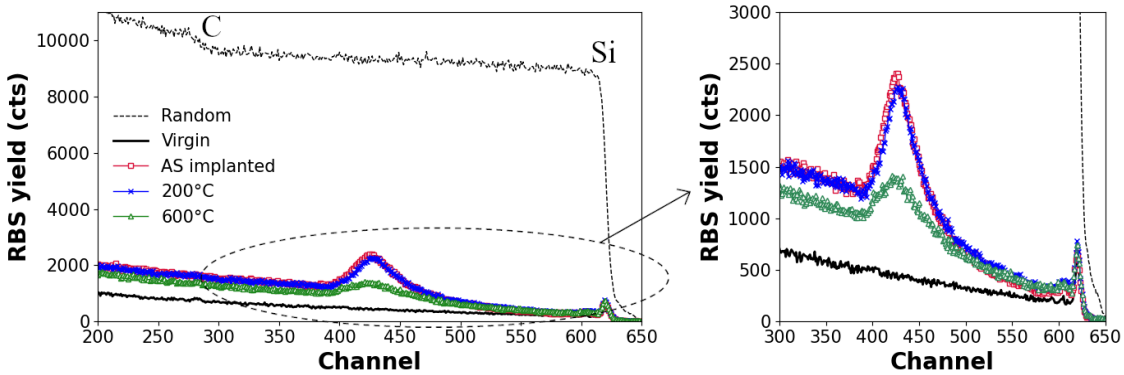

Fig. 1: Channeled-RBS spectra of samples from the first series after anneal at 200°C and 600°C, along with random, un-implanted and as-implanted spectra. The right inset show a magnification on the backscattering yield peaks corresponding to the damaged area.

The same way as for RBS spectra, some preliminary remarks can be made after a glance on the Raman spectra taken on the samples from the first series – presented on Fig. 2. The broad bands from disordered Si-Si, Si-C and C-C phonon are emphasized with dashed areas. They can clearly be seen appearing after ion implantation on the spectrum labelled “RT” (un-annealed). Similarly to channeled RBS characterization, we barely witness any change in the shape of the Raman spectra when the implanted SiC is annealed at 200°C. However, after 400°C anneal and over, the decrease of the broad bands intensities becomes quite noticeable.

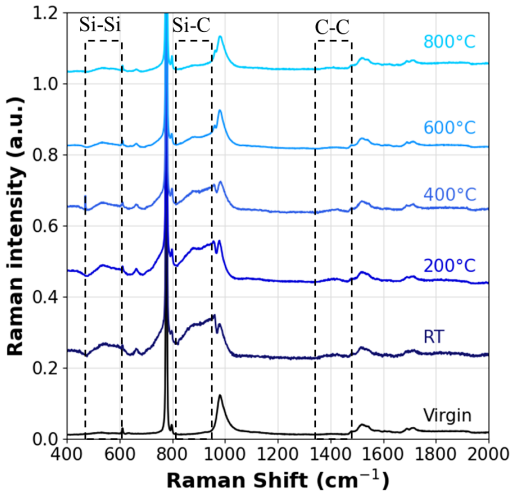

Fig. 2: Raman spectra obtained on all samples from the first series (normalized intensity). The dashed rectangles emphasize the disorder-characteristic Si-Si, Si-C and C-C Raman-active bands.

The Fig. 3a highlights the crystal recovery in the range of RT to 800°C, with data from both characterization techniques. The Raman bands areas were calculated after normalization of the spectra to the TO (E_2) peak, in order to compensate for the loss of intensity due to the increase of the optical absorbance of the disordered material [9], [10]. Both characterization techniques show that the 200°C annealing has almost no effect on the degree of crystallinity of the implanted material. However, both decrease rapidly until 600°C. The Raman bands area points to a residual damage of about 10% of the initial disorder after an 800°C anneal. This result reminds that of Usmann *et al.* [7], who find – after a categorically different implantation process (6H-SiC, Na^+ ions) – very similar kinetics of recovery, although that the initial damage of the SiC lattice was much higher (see Fig. 3b).

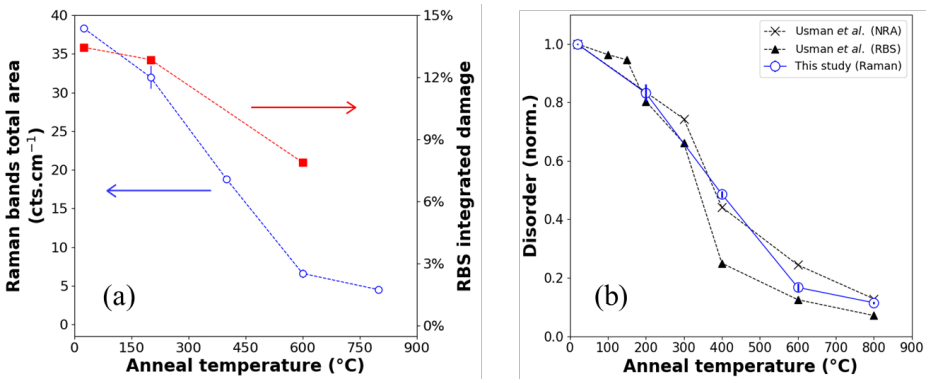

Fig. 3: (a) Raman broad bands amplitude and RBS Si lattice integrated damage (calculated from the method given in [26]) after annealing at different temperatures. (b) Normalized lattice disorder from Raman broad band characterization along with results from Usmann *et al*. [7].

Transferred layer crystal quality. After layer transfer, the crystal quality was investigated using XRD Reciprocal Space mapping (RSM). The light twist angle between the transferred layer crystalline axis and those of the receiver monocrystalline substrate (samples from the second series) allowed to differentiate the (0004) Bragg peaks from both contributions. There is a crucial difference between the pattern obtained on the 950°C anneal sample (Fig. 4a) and those from sample annealed at the three higher temperatures (Fig. 4b to Fig. 4d). The (0004) Bragg peak from the transferred layer align perfectly with that of the substrate as soon as 1300°C, and does not change with the application of more severe annealing. The lattice parameter inferred from these last three measurements is the same than that of the bulk monoSiC (receiver substrate) – proving the full relaxation of the crystal. Contrarily, we find for the first sample an increase in the layer's lattice parameter of 0.18%. The residual presence of hydrogen (assessed with SIMS, see Fig. 5) could be the cause of this strain.

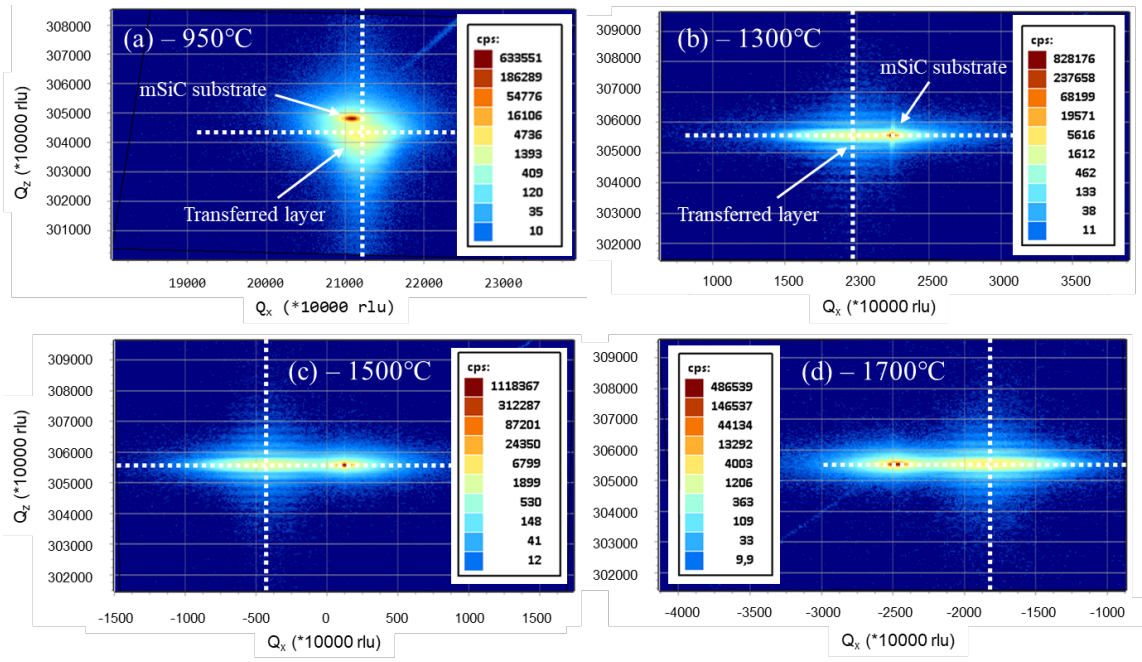

Fig. 4: XRD-RSM of the (0004) 4H-SiC Bragg peak established on samples from the second series after of several annealing temperatures: (a) 950°C; (b) 1300°C; (c) 1500°C and (d) 1700°C.

The Laue fringes, clearly distinguishable on Fig. 4b to Fig. 4d, prove the good quality of the transferred layer after 1300°C. However, they are, in the case of the 950°C annealed sample, not only hardly visible, but also highly asymmetrical along the Q_z cut. This last point emphasizes the existence of an in-depth strain gradient in the transferred layer – which completely disappears after the 1300°C treatment. The width of the rocking curve across the transferred layer's peak is also similar in all the last three measurements, and quite higher in that of the 950°C annealed sample. Such a mosaicity can however come from the presence of extended defects such as dislocations, but is likely to originate from the bonding interface, which may not be fully closed after moderated temperatures annealing.

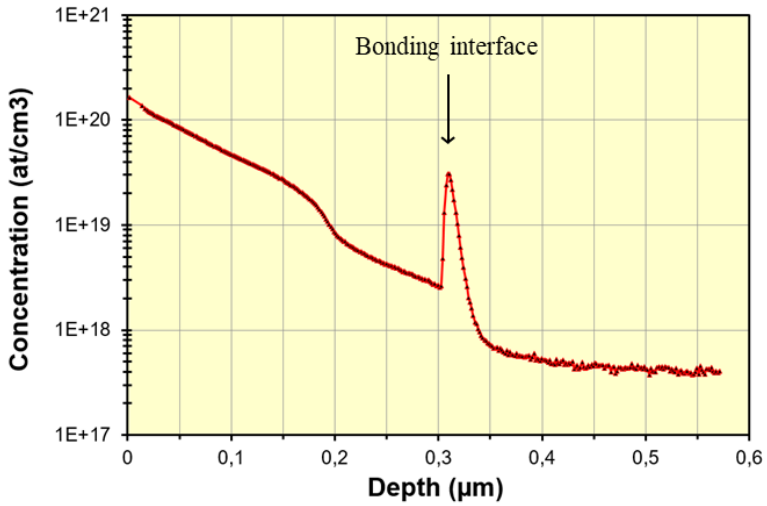

Fig. 5: Hydrogen SIMS profile on a second series sample (950°C anneal).

Dopant reactivation

Since the SiC power devices are vertical conduction devices, the electrical conductivity (and thus, the electrical activation) of the 4H-SiC transferred layer is also an important point to focus on. Two types of electrical measurement were carried out in order to probe the electrical conductivity of this layer: SSRM and I-V measurements; whose results are shown on Fig. 6. Those two characterizations clearly reveal that the transferred layer is insulating after 950°C – almost no current at all flowed through the

substrate in the range of -1 V to 1 V polarization (see Fig. 6b). Contrarily, the structure is conductive after a 1700°C anneal, and the corresponding SSRM micrograph (Fig. 6a) does not show any contrast difference between the transferred layer and the monoSiC receiver. These results coincide well with the previous XRD characterization: the crystal is indeed insulating after 950°C (as it could be inferred from its crystalline quality); and the transferred layer has fully recovered its properties after 1700°C.

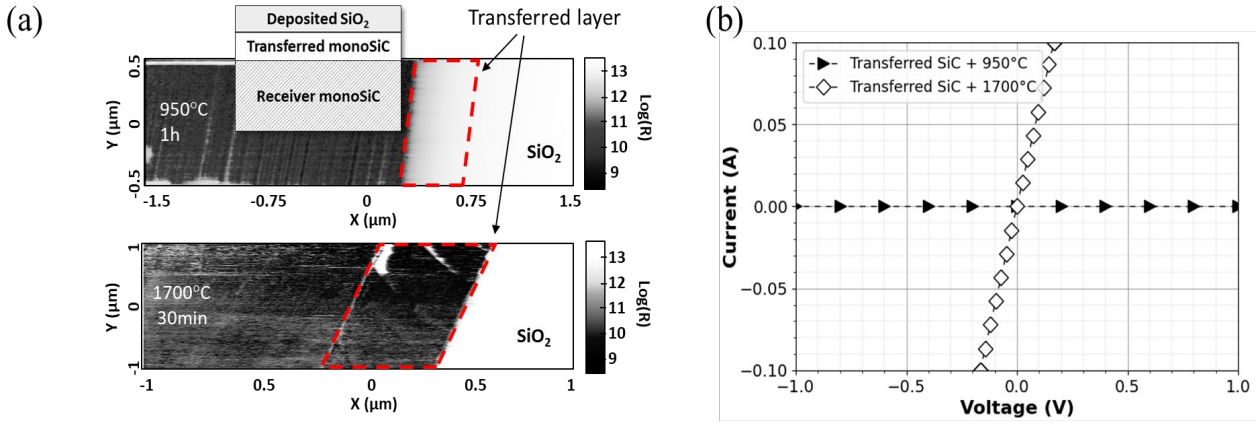

Fig. 6: (a) Cross-section SSRM micrographs from the 950°C and 1700°C anneal samples from the second series. A one µm-thick SiO_2 layer was prior deposited on the front side to allow measuring close to the sample edge. (b) I-V characteristics (carried out on coplanar c-TLM structure on samples from the third series) after anneal at 950°C and 1700°C.

All samples from both the first and the third series were measured using Raman spectroscopy, and the LOPC mode was thoroughly studied in order to understand the ongoing mechanisms under the electrical activity of the H^+-implanted and then transferred 4H-SiC. The Fig. 7 displays the positions of the LOPC peak from all the above-mentioned measurements along with the corresponding active carrier concentrations in the range of 1200°C to 1900°C. The LOPC mode Raman shift shows three distinct steps of recovery over the studied range of temperatures. 1- Between room temperature and 1300°C. In this temperature range, the LOPC Raman mode appears at a frequency lower than that of unintentionally doped 4H-SiC (in other words, below 964.2 cm^{-1} [13]–[15]). The carriers are trapped in the defects of a partly disorganized crystal, such as vacancies or interstitials – which may be complexed with implanted H [4], [23]. The doping concentration in this temperature range could not be estimated from the phonon-plasmon coupling phenomenon, since some parasitic effects may take place. A slight shift of the LO mode Raman shift may indeed occur due to strain, and make such an estimation erroneous. Moreover, the effective conductivity of the material can as well be superior as what the sole doping level would suggest, because of the emergence of other conduction mechanisms such as trap-assisted tunneling. 2- Then, we assist to an explosive dopant activation between 1400°C and 1700°C; suggested by a steep rise in the LOPC peak position. Interestingly, this activation occurs in the same temperature range as that of implanted nitrogen in SiC [17]–[22]. Hence, this phenomenon is more likely related to the diffusion activation energy of nitrogen in SiC rather than to crystal reconstruction mechanisms. 3- Eventually, a 1700°C anneal allows the transferred layer to recover the initial bulk doping level, with no further evolution when annealing up to 1900°C.

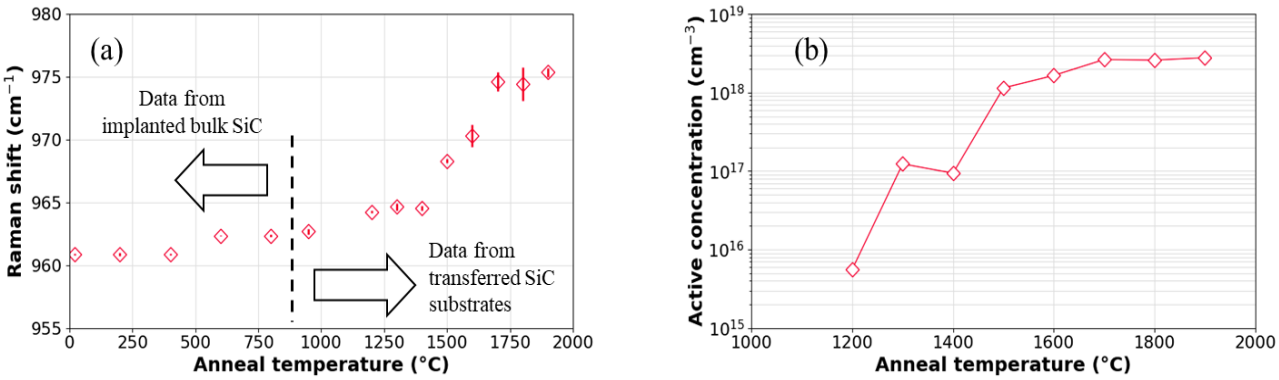

Fig. 7: Electrical activation of implanted and transferred 4H-SiC. (a) Position of the LOPC mode from RT to 1900°C; (b) corresponding active concentration between 1200°C and 1900°C

The electrical activation mechanism is thus proved uncorrelated to the crystal reconstruction process. As shown with XRD, the 4H-SiC lattice fully recovers its quality at 1300°C – namely, at the same temperature the Raman shift of the LO mode regains the position of that of the semi-insulating SiC. Only once the crystal is healed, the dopant reactivation occurs: starting from about 1400°C, and being complete after 1700°C. We can thus conclude that no dopant activation take place in the transferred SiC layer before all (or at least a vast majority of) traps are eliminated through diffusion and recombination from the transferred crystal [23].

Conclusion

We hereby report for the first time studies of healing and reactivation mechanisms of a transferred 4H-SiC thin film over a wide range of temperatures. Raman scattering and RBS – which showed an important crystallinity recovery at relatively low temperatures – could assess the initial influence of the H^+ ion implantation on bulk 4H-SiC crystal. After 950°C, the thin monocrystalline SiC layer is however still insulating. A 1300°C anneal allows the material to fully relax and reorganize, with no further evolution beyond this temperature. The dopant reactivation takes place at higher thermal budgets, after the full recovery of the crystalline quality. The transferred layer then recovers the donor doping level and electrical conductivity after 1700°C. 4H-SiC thin film transfer process optimization can now be carried on using the protocol described here, for instance with the investigation of ion implantation alternatives: such as the dose or the nature of the ions.

Acknowledgement

This project has received funding from the Key Digital Technologies (KDT) under Grant Agreement No 101007237. The KDT receives support from the European Union's Horizon 2020 research and innovation programme and Germany, France, Italy, Sweden, Austria, Czech Republic, Spain.

References

[1] European Commission, *CO_2 emission performance standards for cars and vans*. 2019. [Online]. Available: https://ec.europa.eu/clima/eu-action/transport-emissions/road-transport-reducing-co2-emissions-vehicles/co2-emission-performance-standards-cars-and-vans_en

[2] S. Laferriere *et al.*, "Power SiC: Materials, Devices and Applications 2020," Yole, Market and Technology, 2020.

[3] S. Rouchier, G. Gaudin, and J. Widiez, "150 mm SiC Engineered Substrates for High-voltage Power Devices," *Trans Tech Publ.*, vol. 1062, pp. 131–135, 2021, doi: 10.4028/p-mxxdef.

[4] E. Hugonnard-Bruyère, V. Lauer, G. Guillot, and C. Jaussaud, "Deep level defects in H+ implanted 6H–SiC epilayers and in silicon carbide on insulator structures," *Mat Sci Eng B*, vol. 61–62, pp. 382–388, 1999, doi: 10.1016/S0921-5107(98)00539-X.

[5] G. Irmer, V. V. Toporov, B. H. Bairamov, and J. Monecke, "Determination of the Charge Carrier Concentration and Mobility in n-GaP by Raman Spectroscopy," *Phys State Sol B*, vol. 119, pp. 595–6.3, 1983, doi: 10.1002/pssb.2221190219.

[6] L. Artús, R. Cuscó, J. Ibáñez, N. Blanco, and González-Díaz, "Raman scattering by LO phonon-plasmon coupled modes in n-type InP," *Phys Rev B*, vol. 60, no. 8, pp. 5456–5463, 1999, doi: 10.1103/PhysRevB.60.5456.

[7] M. Usman, M. Nour, A. Yu. Azarov, and A. Hallén, "Annealing of ion implanted 4H–SiC in the temperature range of 100–800 _C analysed by ion beam techniques," *Nuc Inst Methods Phys Res B*, vol. 268, pp. 2083–2085, 2010, doi: 10.1016/j.nimb.2010.02.020.

[8] X. Zhang *et al.*, "Defects in hydrogen implanted SiC," *Nuc Inst Methods Phys Res B*, vol. 436, pp. 107–111, 2018, doi: 10.1016/j.nimb.2018.09.020.

[9] M. Sharma, K. K. Soni, A. Kumar, T. Ohkubo, A. K. Kapoor, and R. Singh, "Blistering kinetics in H-implanted 4H-SiC for large-area exfoliation," *Curr Appl Phys*, vol. 31, pp. 141–150, 2021, doi: 10.1016/j.cap.2021.08.007.

[10] N. Daghbouj *et al.*, "The structural evolution of light-ion implanted 6H-SiC single crystal: Comparison of the effect of helium and hydrogen," *Acta Mater.*, vol. 188, pp. 609–622, 2020, doi: 10.1016/j.actamat.2020.02.046.

[11] Y. S. Katharina, S. Kumar, P. S. Lalshmy, and D. Kanjilal, "Self-organization of 6H-SiC „0001… surface under keV ion irradiation," *J Appl Phys*, vol. 102, p. 044301, 2007, doi: 10.1063/1.2769804.

[12] L. Zhang *et al.*, "Raman study of amorphization in nanocrystalline 3C–SiCirradiated with C+and He+ions," *J Raman Spectr*, vol. 50, no. 8, pp. 1197–1204, 2019, doi: 10.1002/jrs.5631.

[13] M. Chaifal and A. Jaouhari, "Raman scattering from LO phonon-plasmon coupled modes and Hall-effect in n-type silicon carbide 4H–SiC," *J Appl Phys*, vol. 90, p. 5211, 2001, doi: 10.1063/1.1410884.

[14] H. Harima, S. Nakashima, and T. Uemura, "Raman scattering from anisotropic LO phonon–plasmon–coupled mode in n-type 4H– and 6H–SiC," *J Appl Phys*, vol. 78, p. 1996, 1995, doi: 10.1063/1.360174.

[15] J. C. Burton *et al.*, "Spatial characterization of doped SiC wafers by Raman spectroscopy," *J Appl Phys*, vol. 84, p. 6268, 1998, doi: 10.1063/1.368947.

[16] A. Thuaire, "Apport de l'Imagerie Raman et de la Photoluminescence à la Caractérisation de Carbure de Silicium (SiC). Application à l'Étude de Composants Électroniques," [FR], Material Sciences, conducted at Grenoble INP, Grenoble, 2006.

[17] T. Kimoto, N. Inoue, and H. Matsunami, "Nitrogen Ion Implantation into a-SiC Epitaxial Layers," *Phys Stat Sol A*, vol. 162, pp. 263–276, 1997, doi: https://doi.org/10.1002/1521-396X(199707)162:1<263::AID-PSSA263>3.0.CO;2-W.

[18] A. Hallén and M. Linnarsson, "Ion implantation technology for silicon carbide," *Surf Coat Technol*, vol. 306, no. Part A, pp. 190–193, 2016, doi: 10.1016/j.surfcoat.2016.05.075.

[19] V. Simonka, A. Hössinger, J. Weinbub, and S. Selberherr, "Modeling of Electrical Activation Ratios of Phosphorus and Nitrogen Doped Silicon Carbide," in *J Soc Appl Phys*, Kamakura, Japan, 2017. doi: 10.23919/SISPAD.2017.8085280.

[20] C. A. Fisher *et al.*, “An Electrical and Physical Study of Crystal Damage in High-Dose Al- and N-Implanted 4H-SiC,” *Mat Sci Forum*, vol. 897, pp. 411–414, 2017, doi: 10.4028/www.scientific.net/msf.897.411.

[21] M. A. Capano, J. A. Cooper, and M. R. Melloch, “Ionization energies and electron mobilities in phosphorus- and nitrogen-implanted 4H-silicon carbide,” *J Appl Phys*, vol. 87, no. 12, p. 8773, 2000, doi: 10.1063/1.373609.

[22] X. Song, “Activation des dopants implantés dans le carbure de silicium (3C-SiC et 4H-SiC),” [FR], Electronics, conducted at Université François Rabelais de Tours, Tours, 2012. [Online]. Available: https://www.applis.univ-tours.fr/theses/2012/xi.song_3815.pdf

[23] E. Hugonnard-Bruyère, “Etude du comportement électrique des films minces de carbure de Silicium reportés par le procédé improve sur isolant (SiCOI),” [FR], Devices for Integrated Electronics, conducted at INSA Lyon, Lyon, 1999.

[24] D. Chaussende and N. Ohtani, “5 - Silicon Carbide,” in *Single Crystal of Electronic Materials*, Woodhead Publishing in Electronic and Optical Materials., 2019, pp. 129–179. [Online]. Available: https://www.sciencedirect.com/science/article/pii/B9780081020968000057

[25] C. CENBG-Université de Bordeaux, “AIFIRA : Applications Interdisciplinaires des Faisceaux d’Ions en Région Aquitaine,” Scientific Comitee IN2P3, Gradignan, 2020.

[26] J. Xin, “Combining RBS/Channeling, X-ray diffraction and atomic-scale modelling to study irradiation-induced defects and microstructural changes,” Physics, conducted at ED 609 / IRCER, Limoges, 2021. [Online]. Available: https://tel.archives-ouvertes.fr/tel-03219512/file/2021LIMO0017.pdf